Biosensors and Bioelectronics 129 (2019) 132–138

Contents lists available at ScienceDirect

Biosensors and Bioelectronics

journal homepage: www.elsevier.com/locate/bios

Dynamic fluorescent imaging analysis of mitochondrial redox in single cells with a microfluidic device

Qingling Li[a,1], Wei Li[b,1], Shuang Cui[a], Qianqian Sun[a], Haibin Si[a], Zhenzhen Chen[a], Kehua Xu[a], Lu Li[a,*], Bo Tang[a,*]

[a] College of Chemistry, Chemical Engineering and Materials Science, Key Laboratory of Molecular and Nano Probes, Ministry of Education, Collaborative Innovation Center of Functionalized Probes for Chemical Imaging in Universities of Shandong, Institute of Molecular and Nano Science, Shandong Normal University, Jinan 250014, PR China
[b] Department of Hematology, Qilu Hospital, Shandong University, Jinan 250012, PR China

ARTICLE INFO

Keywords:
Mitochondrial redox
Microfluidic
Fluorescence
Single cell

ABSTRACT

The redox balance in cellular mitochondria is closely related to the physiological and pathological processes of the body. When exposed to external stimuli, the redox state in cells changes dynamically, and presents cell heterogeneity, which creates a need for techniques that can make dynamic and reversible visual analysis of redox in mitochondria at single-cell level. Here we describe a method for single-cell redox analysis based on a microfluidic device combing with a reversible fluorescent probe (Cy-O-ebselen), that enables online culture, labelling and dynamic fluorescent imaging analysis of mitochondrial redox (H_2O_2/GSH) change. Using this method, we further explored the dynamic changes of mitochondrial redox state after thermal stimulation or combined thermal-drug stimulation, and analysed the heterogeneous response of cells to external stimuli at the single cell level.

1. Introduction

Intracellular redox and its dynamic balance play an important role in maintaining normal function of organisms. Hydrogen peroxide (H_2O_2) and glutathione (GSH) in cells are most representative molecules in sustaining intracellular redox balance. Their relative cellular level is closely related to the process of cell proliferation, differentiation, apoptosis, disease occurrence and development (Albrecht et al., 2011; Emanuele et al., 2018). However, changes of intracellular redox and its complicated mechanism associated with physiological and pathological results were poorly understood because it was more difficult to measure dynamic changes of intracellular oxidation/reduction (Janssen-Heininger et al., 2000; Murphy et al., 2011). Mitochondrion, as the central site of the eukaryotic cell respiration and apoptosis regulation (Friedman and Nunnari, 2014), is the main source of intracellular H_2O_2. Under physiological conditions, electronics leaking from the electron transport chain react with O_2 in mitochondria to form initial $O_2^{\cdot-}$, and these $O_2^{\cdot-}$ can turn to H_2O_2 with more oxidation ability under the catalysis of superoxide dismutase (SOD). Meanwhile, H_2O_2 can also react with GSH and revert to H_2O (Yu et al., 2012), in which case redox balance of cells can be maintained well through self-repair (Zuo et al., 2015). However, a great amount of H_2O_2 could be produced and accumulated in the mitochondria when the cells were exposed to external stimulus or certain pathologic changes. Excessive H_2O_2 could attack mitochondria, along with the redox change, which result in cellular oxidative damages and various harmful pathologic incidents (lipid peroxidation, mitochondrial dysfunction and apoptosis, etc.) (Islam, 2017). In addition, when the reduction/antioxidation balance was disturbed by environmental factors, GSH depletion or excessive expression in mitochondria could also cause redox changes and result in reduction damage or disease occurrence (Kalinina et al., 2014; Zhang et al., 2012). Therefore, accurate monitor of H_2O_2 and GSH in mitochondria is necessary to understand the cell fate (Nietzel et al., 2018; Panieri et al., 2017). As hyperthermia has been shown to be a powerful treatment or adjuvant to radiotherapy and/or chemotherapy in cancer patients (Maebayashi et al., 2017; Oei et al., 2017) by complicated mechanisms, such as interfering with the repair of therapy-induced DNA damage (Kampinga and Dikomey, 2001), activating heat shock proteins, triggering protein unfolding, finally causing loss of functionality and cell death (Dubois et al., 1991). Whatever the mechanisms, condition of mitochondrial redox (H_2O_2 and GSH) is always a key factor for the cell fate (Yin et al., 2018). Therefore, monitoring the dynamic

* Corresponding authors.
E-mail addresses: liql@sdnu.edu.cn (Q. Li), liwei_medicine@163.com (W. Li), 2503172858@qq.com (S. Cui), 137451782@qq.com (Q. Sun), haibinsi@sdnu.edu.cn (H. Si), zzchen@sdnu.edu.cn (Z. Chen), xukehua@sdnu.edu.cn (K. Xu), lilu5252@163.com (L. Li), tangb@sdnu.edu.cn (B. Tang).
[1] These authors contributed equally.

https://doi.org/10.1016/j.bios.2019.01.005
Received 7 November 2018; Received in revised form 31 December 2018; Accepted 9 January 2019
Available online 11 January 2019
0956-5663/

redox change in cells under thermal or drug-assisted thermal stimulation is very helpful to evaluate the therapeutic effect.

Current measurement of mitochondria H_2O_2 and GSH and related conclusions in biology is mostly based on mitochondrial lysate (Cocheme et al., 2011; Rindler et al., 2016). The obtained results are not completely equal in terms of fate among individual cells (Cai et al., 2006) and consequently neglect heterogeneity and differentiation within the population, thus making single-cell analysis more appealing. What's more, mitochondrial H_2O_2 and GSH may dynamically change associated with external stimuli (Spiller et al., 2010). Therefore, real time and in situ analysis of mitochondrial redox (H_2O_2/GSH) in the single living cell is undoubtedly more attractive in determining function and fate of cells at different stages. As to the measuring technique, in recent years, fluorescent imaging based on different probes has greatly attracted attention of researchers due to its high sensitivity and in situ presentation. However, most research failed to report on dynamic changes and the reversible condition of mitochondrial redox because of the irreversible probes used. Besides, many other restrictive factors, such as small cell scale, lower content of mitochondria H_2O_2/GSH, high-activity and easy transformation features, make mitochondrial redox (H_2O_2/GSH) in single cell extremely difficult to detect. To settle the problem, a fluorescent probe, which can specifically target mitochondria and reversibly react with H_2O_2/GSH with high efficiency is required. What's more, to fulfil the purpose of single-cell analysis, a convenient cell manipulation system is also expected. Owing unique advantages like micron grade-scale space, integrated operation and excellent optical compatibility, microfluidic chip, is becoming one of most promising candidates for single cell research (Heath et al., 2016; Narayanamurthy et al., 2017; Valihrach et al., 2018; Zhang et al., 2011). Considering all above, combining the reversible fluorescent probe and microfluidic chip together is very promising to accomplish real time and in situ analysis of mitochondrial redox (H_2O_2/GSH) dynamic change in single cells (Li et al., 2016; Lin et al., 2011).

In this paper, we propose a microfluidic device to adapt to the single cell analysis, which consists of a microchip, a gravity drive pump, a CO_2-control, a temp-control and a laser scanning confocal microscope unit. Combing this microfluidic device with a reversible fluorescent probe (Cy-O-ebselen, switch on/off), which is characterized by a mitochondrial targeting and selective redox recognition, we have achieved capture/location, online culture, labelling and fluorescent imaging analysis of mitochondrial redox (H_2O_2/GSH) change in single cell under thermal stimulus and combined thermal/N-Ethylmaleimide (NEM) stimulus. On this basis, correlation between redox change and apoptosis degree were studied and heterogeneous response of cells to external stimuli were further analysed.

2. Experimental

2.1. Cell and reagent

MCF-7/MCF-10A cell lines were purchased from Nanjing Keygen Biological Technology Co., LTD (Nanjing, China). High glucose culture medium (DMEM) and 0.25% trypsin-EDTA (1 ×) were obtained from gibco USA. Hoechst 33258, Annexin V-FITC apoptosis kit, N-acetylcysteine (NAC), polylysine (Poly-L-lysine, PLL) total protein extraction kit and mitochondria isolation kit were provided by Beyotime Institute of Biotechnology (Beyotime, Shanghai, China). Cyt c primary antibody was purchased from Santa Cruz company (Santa Cruz Biotechnology, USA). Active caspase-3 primary antibodies were purchased from CST Company (cell signaling Technology, USA). The 3-(4, 5-dimethyl thiazol-2-yl)-2,5-diphenyltetrazolium bromide (MTT) was purchased from Sigma Chemical Company (St. Louis, MO, USA). NEM was purchased from Shanghai Mindray's Chemical Technology Co., LTD (Shanghai, China). The near-infrared reversible fluorescent probe, Cy-O-Eb, was synthesized in our laboratory (Xu et al., 2013). All other reagents used in this study were better than analysis grade unless it has special instructions. Ultrapure water (18.2 MΩ·cm) was supplied by Milli-Q apparatus (Millipore, Bedford, MA, USA), which was disposed by high temperature sterilization before use.

2.2. Microfluidic device operation

Microfluidic chip was initially filled with 75% ethanol solution, and exposed for 15 min under UV irradiation. Ethanol within the microchannel was then replaced with PBS buffer solution, at the same time 0.1 mg/ml poly lysine was added to microchamber, after which it was put in incubator to incubate for 30 min. Finally the microchannel was flushed with culture medium. Thermal stimulus on microfluidic chip was carried out as required. Replacement of culture medium, transmission of cell suspension and introduction/export of the probe were operated by gravity driven mode through adjusting height difference of liquid surface in horizontal stock liquid pool and chip waste reservoir, and the process was monitored by the fluorescence microscopy. The device needs only 20 s to completely finish solution replacement in the microchannel.

Cells were digested in 0.25% trypsin at logarithmic phase. Then cell suspension with a density of 5×10^6–1×10^7 /ml was added to horizontal stock liquid pool. The microchamber can provide cell location and cell culture for a long time.

Cy-O-Eb probe dissolved in DMSO (5 μM) was added to horizontal stock reservoir after MCF-7 cell growing on glass coverslips. Regulating of liquid level difference was as expatiated above to accomplish probe incubation.

2.3. Mitochondrial redox (H_2O_2/GSH) imaging

Thermal (42 °C–46 °C) or combined thermal/NEM (43 °C, NEM: 1 μM, 30 μM or 100 μM) stimulus kept its respective temperature for 1 h on the microfluidic chip. Next, the temperature was adjusted to 37 °C for further cell culture. Confocal fluorescence imaging was performed on a Leica TCS SP5 laser scanning confocal microscope and a 20 × or 40 × objective lens. The cells were excited by a He-Ne laser (633 nm) and the fluorescence was collected with a PMT detector from 650 nm to 800 nm.

2.4. Nuclear staining, FCM and western blot

Nuclear staining of MCF-7 cells was done 6 h after the 1 h thermal stimulus. Hoechst 33258 with the final concentration of 2 μg/ml was added and cells were incubated for 10 min. Fluorescence imaging for nucleus was carried out on the microchip by laser scanning confocal microscope with a 40 × objective lens and the excitation/emission wavelength at 405 nm/430–550 nm.

For flow cytometry, 1×10^6/ml cells were washed with PBS and resuspended in 1 × binding buffer. Annexin (V-FITC) and propidium iodide (PI, 5 mg/ml) were added then. The analysis was performed on a flow cytometer (Shanghai Fuchang Technology CO., LTD, Shanghai, China).

For western blot, extraction of total protein was used to measure the active caspase 3. Mitochondria was separated from MCF-7 cells and this mitochondria-free cytoplasm was further used for determination of Cyt c. After quantitation (active caspase-3, 30 μg; Cyt c, 50 μg), both kinds of protein became degeneration after boiling for 5 min, and then the sample was kept on ice. After gel electrophoresis, exposure etc, analysis of optical density value was obtained by gel imaging and gray analysis software.

3. Results and discussion

3.1. Reversible reaction mechanism of Cy-O-Eb probe

To facilitate dynamic analysis of intracellular mitochondrial redox,

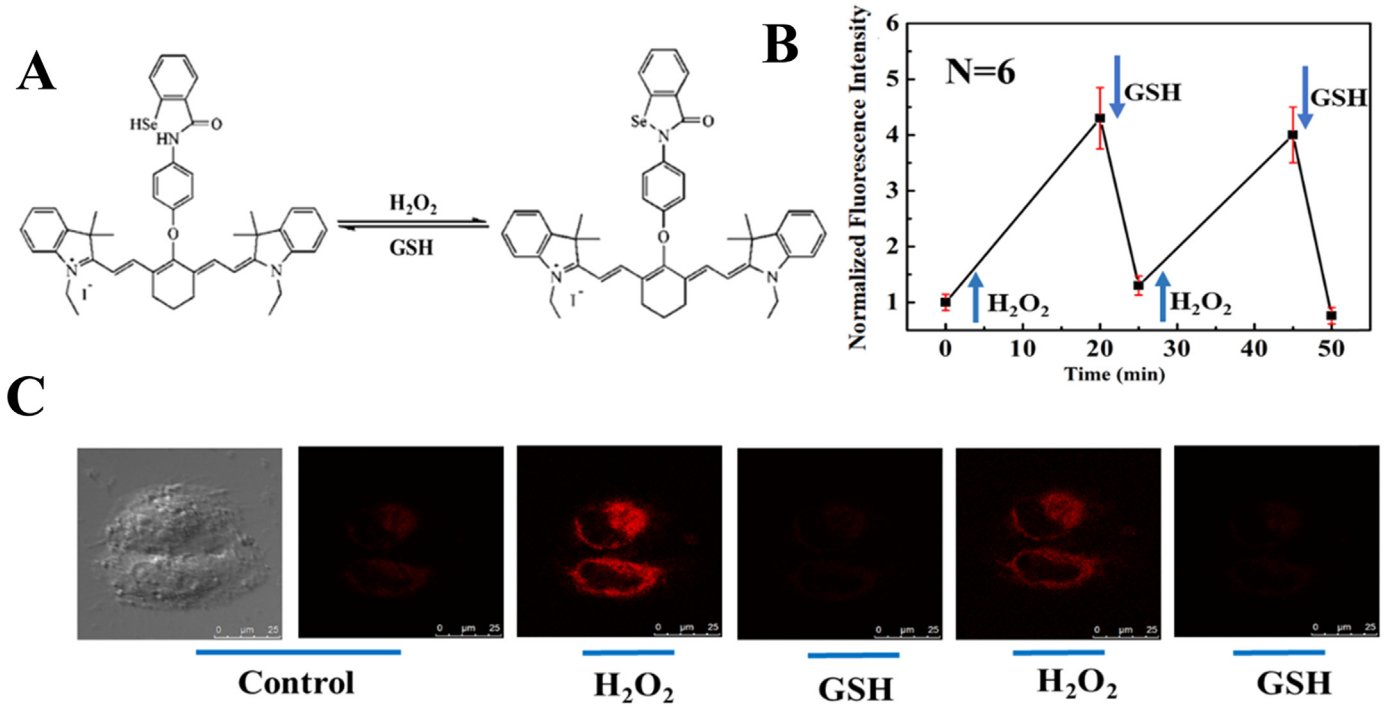

Fig. 1. Reversible reaction of the Cy-O-Eb probe. (A) Switching on/off mechanism of the reversible reaction with H_2O_2/GSH. (B) Representative fluorescent imaging of the Cy-O-Eb probe under different conditions. (C) Quantitative fluorescent analysis of Cy-O-Eb probe under different conditions.

a near-infrared reversible fluorescent probe Cy-O-Eb by our group was used as a fluorescent on-off switch to present the level of H_2O_2 and GSH (Xu et al., 2013). The structure of the probe is shown in Fig. 1A. When the probe reacts with GSH, the bond selenium-nitrogen (Se-N) in the Cy-O-ebselen part of the probe can specifically identify thiol of GSH, resulting in fluorescence quenching. On the other hand, the five-membered ring of the Cy-O-ebselen part can be closed when the probe reacts with H_2O_2, recovering the red fluorescence. To demonstrate the reversible response of the probe, we recorded the dynamic fluorescent changes of cells under different conditions after incubated with our probe (Fig. 1B, C). When 200 μM H_2O_2 solution was added into the cells, the fluorescent intensity was found to rise slowly. When adding 20 μM GSH, the fluorescence of cells could decline rapidly. Following the same operation above, the next cycle begins again when the fluorescent intensity of the probe recovers to the baseline. According to the result, we can clearly see the probe showing a great reversible response on the redox molecule pair of H_2O_2/GSH. The probe also showed mitochondrial targeting ability, high selectivity to H_2O_2 and GSH, and high sensitivities (Xu et al., 2013). The thermal stability of probe under different temperature was further tested and it showed the fluorescence of the probe maintained consistency between 36.5 °C and 46 °C under the same redox state (Fig. S1).

3.2. Microfluidic device characterization

For high efficient single-cell analysis, we developed a microfluidic device, which consists of a microchip, a gravity drive pump, a CO_2-control, a temp-control and a laser scanning confocal microscope unit (Fig. 2A). The microfluidic chip was designed to contain four microchannel branches and 3 microchambers for each branch (Fig. 2B). Each microchamber (long, 500 μm; width, 380 μm; high, 40 μm) was used for cell capture, location, culture, fluorescence labelling and imaging analysis. The gravity drive pump, as a key auxiliary, was used for introduction of cells and reagent. Stepping motor and its connecting screw rotation were operated to drive up or down of the horizontal stock liquid pool, so that the level difference between the stock pool and the waste pool on chip could emerge gradually, in which case a constant flow velocity could be achieved. Meanwhile, temperature correction (Fig. S2) was carried out in case of temperature gradient between heater and microchambers, which could obtain a real temperature in the process of cell culture, online-labelling and thermal stimulus. Next, online-labelling and longer culture for cells on chip were accomplished by selection and optimization of CO_2-control parameters.

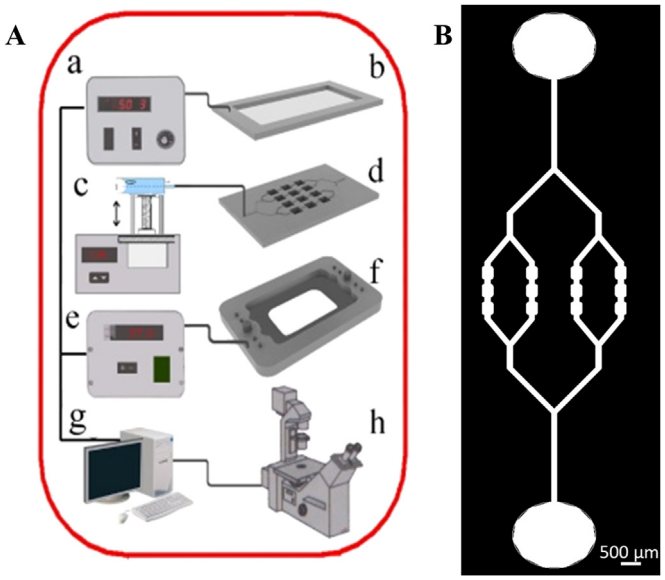

Fig. 2. The microfluidic device. (A) Sketch map of the microfluidic device and ancillary facility: CO_2 control (a, b), skeleton diagram of gravity-drive pump (c), microfluidic chip (d), temperature control (e), heater (f) and confocal imaging system (g, h). (B) Schematic diagram of the microchip.

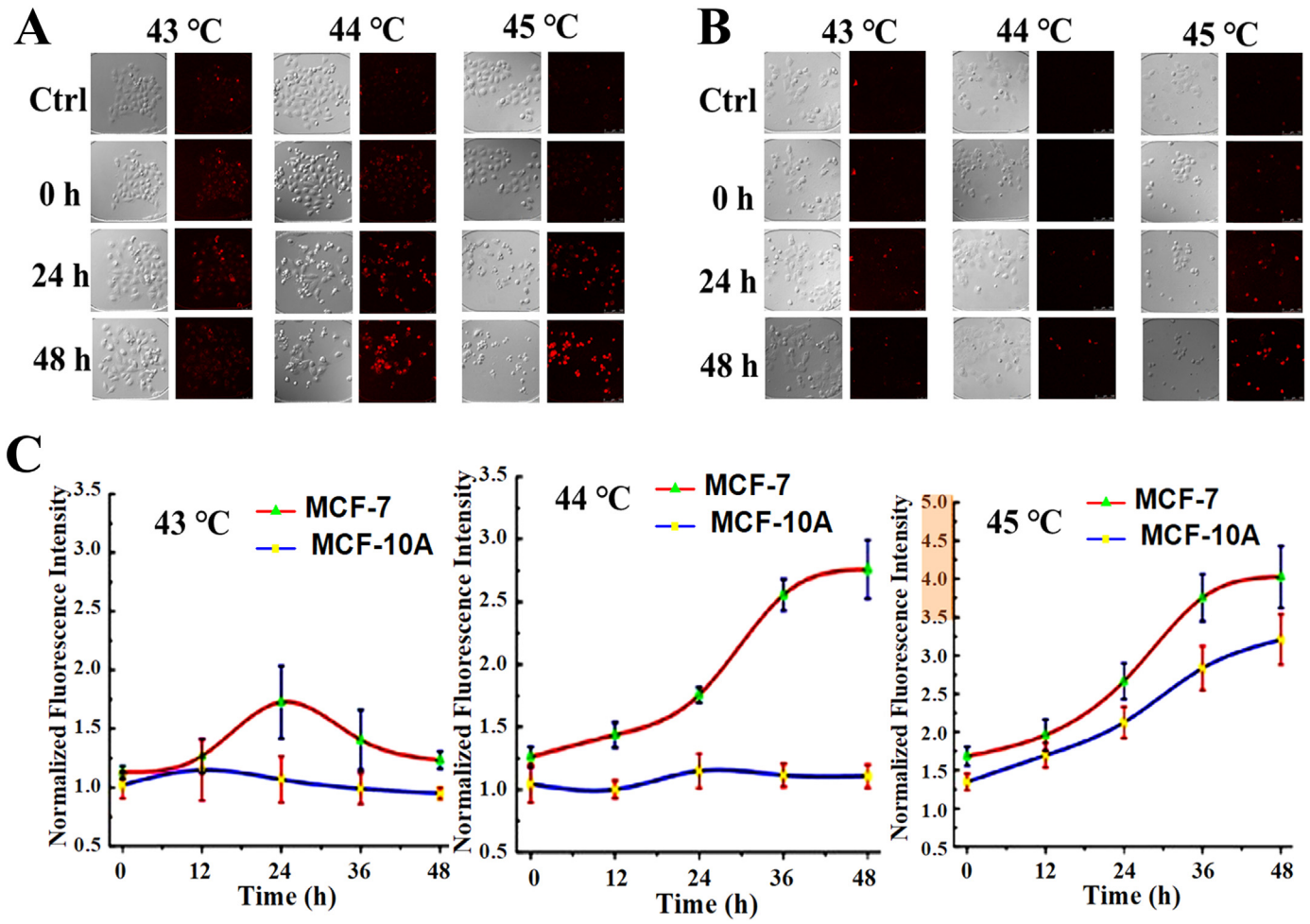

Fig. 3. Imaging analysis of mitochondrial redox state in MCF-7 cells (A) and in MCF-10A cells (B) after thermal stimulus. Ctrl, control, cells before any thermal stimulus. (C) Fluorescent intensity curve of mitochondrial redox change.

3.3. Imaging of mitochondrial redox (H_2O_2/GSH) in MCF-7/MCF-10A cell

Next, the microfluidic device above was tested for detecting the redox state in cellular mitochondria after different thermal stimulus. We carried out a long-term observation after the stimulus in order to get dynamic information of cellular redox change. Given a thermal stimulus at 43 °C for 1 h, fluorescent intensity of MCF-7 cells slowly increased within 24 h and then decreased, indicating the redox went to oxidation state first, and returned to redox homeostasis. However, with the stimulus at 44 °C, we could only see the fluorescent increase within 48 h, which suggested no reversion after the oxidation. Similar changes could also be observed at 45 °C (Fig. 3A, C). However, MCF-10A seemed to be more reluctant to the thermal stimulus: 43 °C and 44 °C could not cause significant redox changes and only 45 °C stimulated some level of oxidation (Fig. 3B, C).

Based on the results above, single cell analysis of mitochondrial redox change was performed in order to further understand single cell behaviour among MCF-7 cell clusters. Similarly, thermal stimulus at 43 °C could lead individual cells turning to oxidation state till reaching the maximum, and then started to drop from there, indicating the cell turning to reduction state (Fig. 4A, B), which was a typical example of the experimental results we observed above (Fig. 3A). We also checked 44 °C and 45 °C stimulus on individual cells, and got the consistent phenomenon as in Fig. 3A. Moreover, we could clearly see a number of vesicular and gemmiform protrusions from the cell surface, which indicated the beginning of apoptosis (Fig. 4A). Besides, we performed a short-term observation on single MCF-7 cells after 1 h thermal stimulus, at 37 °C, 42–46 °C, respectively. Imaging of mitochondrial redox state in single cells was explored with the help of the device 0, 1 or 2 h later, which showed that within a comparatively short duration, only higher temperature like 45 °C or 46 °C, could change the mitochondrial redox level of some cells (Fig. 4C). Moreover, there were individual exceptional cells less active facing the same stimulus, which suggested that heterogeneity existed in the same kind of cells under the same physiological state.

3.4. Apoptosis evaluation of MCF-7 cells under the same thermal stimulus by other biological methods

Next, we checked the apoptotic status of MCF-7 cells under the same thermal stimulus via nuclear staining, FCM and western blot. Experimental result of nuclear staining of MCF-7 cells induced by thermal stimulus was shown in Fig. 5A. It shows that 6 h after the 1 h 44 °C stimulus, nucleus began to appear concentrated and irregular. Under 45 °C stimulus for 1 h, nuclear chromatin showed obvious edge set and enrichment, at the same time, cell surface was starting to bubble as results of cell falling off and forming apoptotic body with membrane package at 21 h. Using FCM to detect apoptosis rate of MCF-7 cells with the same stimulus (Fig. 5B), the flow results indicated that the apoptotic rate and death rate of MCF-7 cells increased with the temperature increase. Protein expression of Cyt-C and active caspase-3 in cytoplasm of MCF-7 cells also rise under thermal stimulus (Fig. 5C). Once heating load applied to the MCF-7 cell was higher than 44 °C, Cyt-C began to show elevated expression; and active caspase-3 started to increase at

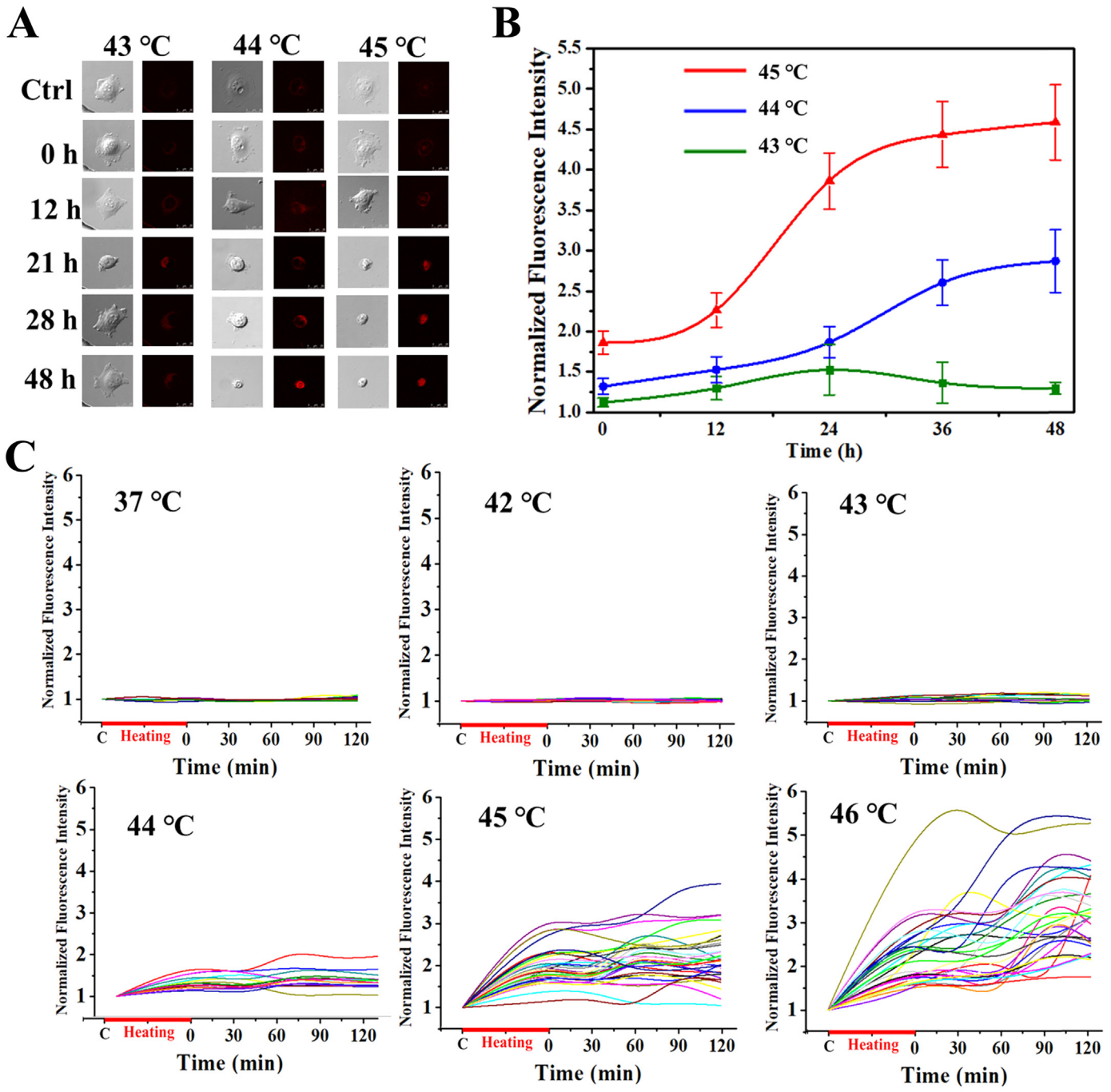

Fig. 4. Dynamic analysis of mitochondrial redox change in single MCF-7 cells (0–48 h) induced by thermal stimulus. (A) Typical imaging on mitochondrial redox in single MCF-7 cells (long-term observation). Ctrl, control, cells without any thermal stimulus. (B) Fluorescent intensity curve of cell mitochondrial redox change using data of 20 individual cells analysis at each temperature (long-term observation). (C) Fluorescent intensity curve of single cell mitochondrial redox change at conditions of different thermal stimulus (short-term observation). Each curve shows variation trend of redox for one cell.

45 °C. At higher 46 °C, both proteins obviously showed excessive expression. All three biological results indicated different levels of apoptosis with different thermal stimulus, respectively. Combined with the results from Figs. 3 and 4, it could be concluded that mitochondrial redox dynamic variation was closely related to cell apoptosis, which made our fluorescent imaging analysis another potential method for apoptotic evaluation.

3.5. Application of mitochondrial redox assay

Lots of anticancer drugs can induce the generation of reactive oxygen species in mitochondria. Precious study has shown that with or without L-buthionine sulphoximine (BSO), an inhibitor of γ-glutamyl cysteine-synthase, the redox status could obviously change in HepG2 and HL7702 cellular mitochondria (Xu et al., 2013, Figs. 5 and 6). N-Ethylmaleimide (NEM), a K^+-Cl^-cotransport activator, was reported to induce apoptosis in a dose-dependent manner in HepG2 cells (Kim et al., 2001a). One of its known mechanisms is by elevating intracellular level of reactive oxygen species (Kim et al., 2001b). Another study demonstrated that glutathione system imbalance and reduced redox potential caused by NEM could further induce programmed death in MCF-7 cells (Shakhristova et al., 2016). We then attempted to

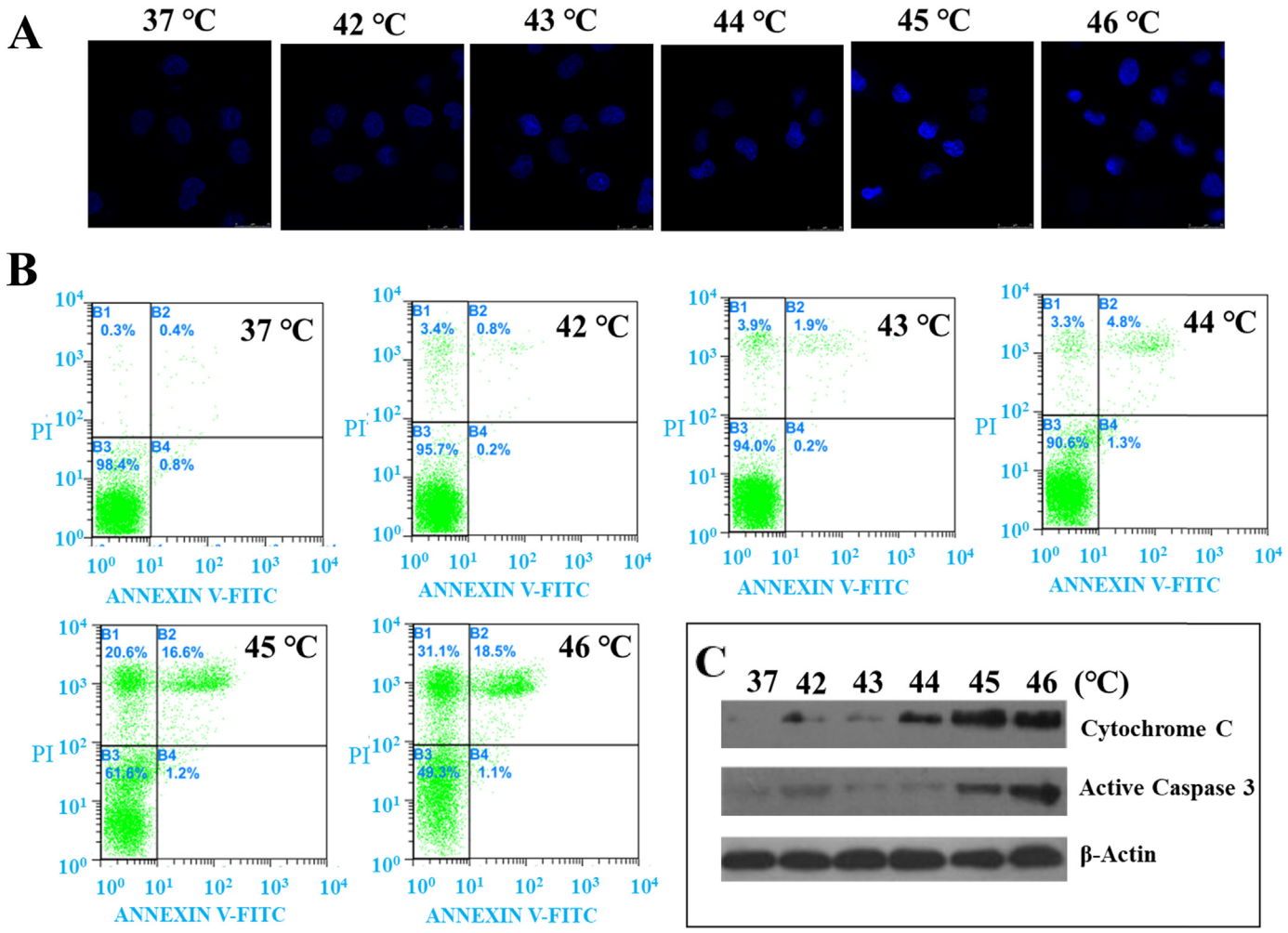

Fig. 5. Apoptosis evaluation of MCF-7 cells under thermal stimulus. (A) Nuclear staining of cells induced by different heat dosage. (B) Flow cytometry map. (C) Expression of Cyt-C and active caspase-3 after cell induced by thermal stimulus.

explore the combination effect of NEM and thermal stimulus on cellular mitochondrial redox homeostasis. At 43 °C, NEM at different concentrations (1 μM, 30 μM, 100 μM) was added to MCF-7 cells respectively, and then dynamic tracking on redox change was carried out by our method. Different from the result above at 43 °C, redox change turned to oxidation state obviously (Fig. 6A, B). When concentration of NEM increased to 30 μM, most of the MCF-7 cells appeared to be apoptotic (Fig. 6A). MTT test further examined the precise NEM dosage on cell proliferative inhibition ratio under the condition of NEM-thermal stimulus. From Table S1, it can also be clearly seen that MCF-7 cells have a dose-dependent sensitivity of NEM. Therefore, dynamic monitoring mitochondrial redox can provide a simple and rapid method of determining temperature for thermal therapy with drug auxiliary and the optimum dose.

4. Conclusions

Combining a laboratory-synthesized, reversible fluorescent probe (Cy-O-ebselen) with a microfluidic device, we have developed a new method to achieve real-time fluorescent imaging analysis of mitochondrial redox change in single cells. Using this method, we explored the dynamic changes of mitochondrial redox state under thermal or combined thermal-drug stimulation, and analysed the heterogeneous response of cells to external stimuli at single cell level. We also investigated the relationship between mitochondrial redox dynamic change and cell apoptosis by flow cytometry and Western blot. We anticipate the proposed method will offer a convenient platform for the study of cellular redox and cell functions responding to external stimuli.

CRediT authorship contribution statement

Qingling Li: Conceptualization, Data curation. **Wei Li:** Formal analysis, Writing - original draft. **Shuang Cui:** Validation. **Qianqian Sun:** Investigation. **Haibin Si:** Software. **Zhenzhen Chen:** Visualization. **Kehua Xu:** Resources, Supervision. **Lu Li:** Methodology, Funding acquisition, Writing - review & editing. **Bo Tang:** Funding acquisition, Project administration, Resources.

Acknowledgements

This work was supported by the National Natural Science Foundation of China (21535004, 91753111, 21675104 and 21675102), the Key Research and Development Program of Shandong Province (2018YFJH0502), the Natural Science Foundation of Shandong Province of China (ZR201709200224, ZR2016JL008, ZR2016BM02), and China Postdoctoral Science Foundation (2016M602179, 2017T100510).

Conflicts of interest

There are no conflicts to declare.

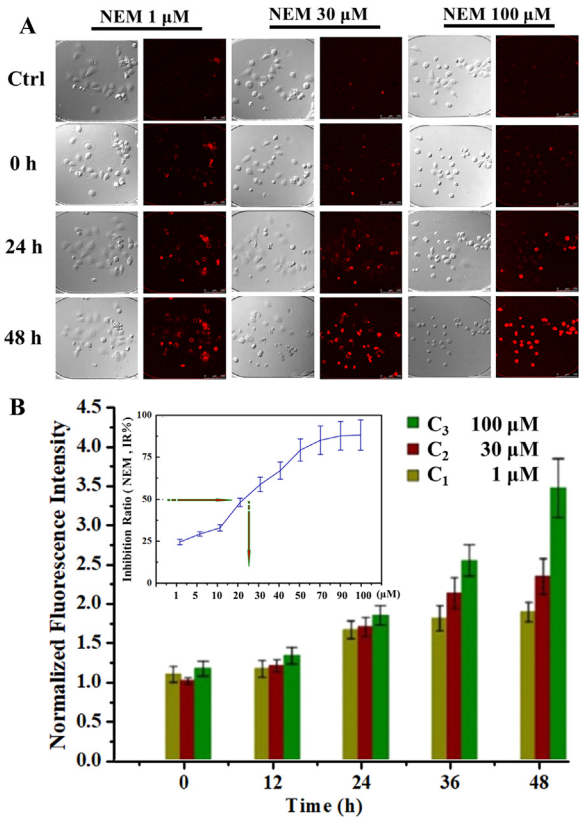

Fig. 6. Analysis of mitochondrial redox and apoptotic features of MCF-7 cells induced by the combined thermal-NEM stimulus. (A) Fluorescent imaging was taken after cell being treated with hyperthermia (43 °C, 1 h) in the presence of NEM (1 μM, 30 μM and 100 μM). (B) Statistical analysis based on normalized fluorescent intensity of MCF-7 cells.

Appendix A. Supplementary material

Supplementary data associated with this article can be found in the online version at doi:10.1016/j.bios.2019.01.005.

References

Albrecht, S.C., Barata, A.G., Grosshans, J., Teleman, A.A., Dick, T.P., 2011. Cell. Metab. 14, 819–829.
Cai, L., Friedman, N., Xie, X.S., 2006. Nature 440, 358–362.
Cocheme, H.M., Quin, C., McQuaker, S.J., Cabreiro, F., Logan, A., Prime, T.A., Abakumova, I., Patel, J.V., Fearnley, I.M., James, A.M., Porteous, C.M., Smith, R.A., Saeed, S., Carre, J.E., Singer, M., Gems, D., Hartley, R.C., Partridge, L., Murphy, M.P., 2011. Cell. Metab. 13, 340–350.
Dubois, M.F., Hovanessian, A.G., Bensaude, O., 1991. J. Biol. Chem. 266, 9707–9711.
Emanuele, S., D'Anneo, A., Calvaruso, G., Cernigliaro, C., Giuliano, M., Lauricella, M., 2018. Chem. Res. Toxicol. 31, 201–210.
Friedman, J.R., Nunnari, J., 2014. Nature 505, 335–343.
Heath, J.R., Ribas, A., Mischel, P.S., 2016. Nat. Rev. Drug. Discov. 15, 204–216.
Islam, M.T., 2017. Neurol. Res. 39, 73–82.
Janssen-Heininger, Y.M., Poynter, M.E., Baeuerle, P.A., 2000. Free. Radic. Biol. Med. 28, 1317–1327.
Kalinina, E.V., Chernov, N.N., Novichkova, M.D., 2014. Biochemistry 79, 1562–1583.
Kampinga, H.H., Dikomey, E., 2001. Int. J. Radiat. Biol. 77, 399–408.
Kim, J.-A., Kang, Y.S., Lee, Y.S., 2001a. Eur. J. Pharmacol. 418, 1–5.
Kim, J.-A., Kang, Y.S., Park, S.H., Kim, H.W., Cho, S.-Y., Lee, Y.S., 2001b. Eur. J. Pharmacol. 433, 1–6.
Li, Q., Chen, P., Fan, Y., Wang, X., Xu, K., Li, L., Tang, B., 2016. Anal. Chem. 88, 8610–8616.
Lin, C., Kolossov, V.L., Tsvid, G., Trump, L., Henry, J.J., Henderson, J.L., Rund, L.A., Kenis, P.J., Schook, L.B., Gaskins, H.R., Timp, G., 2011. Integr. Biol. 3, 208–217.
Maebayashi, T., Ishibashi, N., Aizawa, T., Sakaguchi, M., Sato, T., Kawamori, J., Tanaka, Y., 2017. Oncol. Lett. 13, 4959–4964.
Murphy, M.P., Holmgren, A., Larsson, N.G., Halliwell, B., Chang, C.J., Kalyanaraman, B., Rhee, S.G., Thornalley, P.J., Partridge, L., Gems, D., Nystrom, T., Belousov, V., Schumacker, P.T., Winterbourn, C.C., 2011. Cell. Metab. 13, 361–366.
Narayanamurthy, V., Nagarajan, S., Firus Khan, Aa.Y., Samsuri, F., Sridhar, T.M., 2017. Anal. Methods 9, 3751–3772.
Nietzel, T., Elsasser, M., Ruberti, C., Steinbeck, J., Ugalde, J.M., Fuchs, P., Wagner, S., Ostermann, L., Moseler, A., Lemke, P., Fricker, M.D., Muller-Schussele, S.J., Moerschbacher, B.M., Costa, A., Meyer, A.J., Schwarzlander, M., 2018. New. Phytol.
Oei, A.L., Vriend, L.E., Krawczyk, P.M., Horsman, M.R., Franken, N.A., Crezee, J., 2017. Int. J. Hyperth. 1–12.
Panieri, E., Millia, C., Santoro, M.M., 2017. Free. Radic. Biol. Med. 109, 189–200.
Rindler, P.M., Cacciola, A., Kinter, M., Szweda, L.I., 2016. Am. J. Physiol.-Heat C 311, H1091–H1096.
Shakhristova, E.V., Stepovaya, E.A., Ryazantseva, N.V., Nosareva, O.L., Yakushina, V.D., Ivanov, V.V., Novitskii, V.V., 2016. Bull. Exp. Biol. Med. 160, 364–367.
Spiller, D.G., Wood, C.D., Rand, D.A., White, M.R., 2010. Nature 465, 736–745.
Valihrach, L., Androvic, P., Kubista, M., 2018. Int. J. Mol. Sci. 19.
Xu, K., Qiang, M., Gao, W., Su, R., Li, N., Gao, Y., Xie, Y., Kong, F., Tang, B., 2013. Chem. Sci. 4, 1079–1086.
Yin, W., Bao, T., Zhang, X., Gao, Q., Yu, J., Dong, X., Yan, L., Gu, Z., Zhao, Y., 2018. Nanoscale 10, 1517–1531.
Yu, F., Li, P., Song, P., Wang, B., Zhao, J., Han, K., 2012. Chem. Commun. 48, 4980–4982.
Zhang, H., Limphong, P., Pieper, J., Liu, Q., Rodesch, C.K., Christians, E., Benjamin, I.J., 2012. FASEB J. 26, 1442–1451.
Zhang, X., Li, Q., Chen, Z., Li, H., Xu, K., Zhang, L., Tang, B., 2011. Lab Chip 11, 1144–1150.
Zuo, L., Zhou, T., Pannell, B.K., Ziegler, A.C., Best, T.M., 2015. Acta Physiol. 214, 329–348.